Journal of Computers Vol. 36 No. 5, October 2025, pp. 281-297
https://doi.org/10.63367/199115992025103605019

A Deep Learning-Driven Optimization Method for Automotive Hood Stamping Die Parameters and Springback Compensation

Li-Hua Hu[1,2*], Feng Yang[1], Wen-Ya Shi[1],
Tao Wang[1], and Hao Gu[1]

[1] Department of Mechanical Engineering, Hebei Institute of Mechanical and Electrical Technology,
Xingtai City 054000, Hebei Province, China
{hulihua890210, yangfeng5978, 18903199996,
wangtao1234562025, guhao1234562025}@163.com

[2] Digital Technology Innovation Center for Mechanical Manufacturing Process,
Xingtai City 054000, Hebei Province, China

Received 1 August 2025; Revised 22 September 2025; Accepted 7 October 2025

Abstract. The stamping of automotive hoods presents significant challenges due to their complex geometry and inherent springback issues. Therefore, die parameter optimization is crucial to achieving high-quality forming. This study proposes a deep learning-driven framework that combines a predictive model with finite element simulation and experimental verification to address these challenges. This approach significantly improves springback prediction accuracy, enables systematic optimization of die parameters, and reduces reliance on time-consuming trial-and-error methods. Results demonstrate that this approach not only improves forming quality and production efficiency but also provides a practical and academically significant strategy for springback compensation in automotive hood stamping.

Keywords: deep learning, stamping die, automotive hood, parameter optimization, springback compensation

1 Introduction

1.1 Research Background

With increasingly stringent requirements for energy efficiency, environmental sustainability, and vehicle performance, lightweighting has become a key development direction in the automotive industry [1]. As a critical exterior component, the hood panel must not only meet structural and safety standards but also provide excellent surface quality for subsequent painting and assembly [2]. However, due to its large surface area and complex curved shape, stamping hood panels presents significant challenges in achieving dimensional accuracy and surface integrity [3]. A major technical challenge in the stamping of such panels is springback, the phenomenon in which the formed sheet deviates from the intended geometry after unloading due to elastic recovery of the material. Springback not only affects assembly accuracy, but also increases rework costs and prolongs product development cycles. Therefore, optimizing die design parameters is crucial to controlling springback and ensuring dimensional accuracy of hood panels [4]. Developing effective parameter optimization and springback compensation strategies is of great significance to both industrial practice and academic research.

1.2 Literature Review

The literature review provides an overview of recent advances in the field of process optimization, with a particular focus on forming processes and their computational modeling. These technological advances are crucial for improving manufacturing efficiency and product quality. The analysis of this field reveals a multidisciplinary approach that combines traditional optimization methods with cutting-edge artificial intelligence (AI) and deep learning technologies to address the challenges inherent in process optimization. Tully et al. [5] started with tra-

* Corresponding Author

ditional optimization methods and highlighted the effectiveness of combining design of experiments (DOE) with traditional methods to improve the yield of potassium sorbate production. This combination demonstrated the robustness of DOE in enhancing process results through systematic experimentation. Similarly, Sarıkaya et al. [6] used response surface methodology (RSM) to optimize CNC milling parameters for mild steel, highlighting the ability of RSM to handle the complex relationship between multiple process variables and final product quality. The application of RSM is further exemplified in the study of Pan et al. [7], which combined it with advanced microstructural characterization techniques to optimize the properties of red mud-slag composite cementitious materials, demonstrating the versatility of RSM in material optimization. At the forefront of integrating AI into process optimization, Chakraborti's research [8] proposed a comprehensive framework that combines AI with traditional statistical methods, emphasizing that in high-tech manufacturing, the utility of traditional methods will be enhanced when AI complements them for dynamic and continuous optimization. In addition, Liu et al. [9] made a significant contribution to the integration of AI for real-time process analysis and optimization by optimizing the asymmetric channel chain die forming process through an image-based machine learning approach. This approach marks the transition of AI to practical applications in manufacturing processes, meeting the urgent need for adaptable and efficient optimization strategies. Despite these advances, some research gaps remain, especially in the generality of AI models, computational cost, and accurate modeling of springback during the forming process. Accurate springback modeling remains elusive, and innovative solutions that can accurately predict and mitigate this phenomenon are urgently needed to ensure the dimensional accuracy of manufactured parts. At the same time, the study highlights the transformative potential of integrating traditional and modern optimization techniques for manufacturing process improvement. Nevertheless, the literature also emphasizes the need for further improvements to address the identified gaps, especially to ensure computational efficiency and model generality while fully leveraging the potential of artificial intelligence. Therefore, future efforts should be devoted to developing holistic models that combine the precision of traditional methods with the adaptability and efficiency of artificial intelligence, thus leading to new horizons in manufacturing process optimization.

1.3 Research Objectives and Contributions

In this study, a deep learning-driven optimization framework for automotive hood stamping die design is proposed, focusing on parameter optimization and springback compensation. The overall goal is to overcome the limitations of traditional trial-and-error and simulation-based approaches by integrating predictive models, advanced optimization strategies, and experimental validation into a unified workflow. First, a data-driven deep learning model is developed to accurately capture the highly nonlinear and multidimensional relationship between stamping die parameters (e.g., blank holder force, die radius, drawbead configuration, and friction conditions) and the resulting hood springback behavior. Second, a hybrid optimization framework is established that combines the trained deep learning model with a metaheuristic algorithm and finite element simulation to systematically optimize process parameters, reduce computational cost, and accelerate convergence to the optimal solution. Third, using an industrial hood panel as an example, the effectiveness and engineering applicability of the proposed approach are verified under real production conditions. The main contributions of this study can be summarized as follows: (1) A deep learning-based springback prediction model was developed, which significantly improved the prediction accuracy compared with traditional machine learning and pure finite element methods; (2) A hybrid optimization framework integrating data-driven prediction, finite element simulation, and intelligent search algorithms was established, which can achieve efficient and robust parameter optimization under multiple constraints; (3) Industrial case studies showed that the framework can effectively improve forming quality, reduce springback deviation, minimize design iterations, shorten the overall product development cycle, and provide academic value and practical significance for automotive panel manufacturing.

2 Methodology

This framework integrates finite element simulation, deep learning surrogate models, optimization algorithms, and springback compensation into a closed-loop process. It aims to provide both theoretical rigor and engineering practicality for optimizing automotive hood stamping die parameters.

2.1 Overall Workflow

The overall approach can be divided into five main stages: Data Generation: Finite element simulation of the hood stamping process is combined with selected experimental measurements to construct a comprehensive dataset for calibration and validation in Fig. 1. Feature Processing: Material, geometry, and process parameters are normalized and converted into meaningful descriptors that serve as input to the predictive model. Deep Learning Surrogate Model: A multi-task neural network is trained to capture the highly nonlinear mapping between process parameters and forming quality metrics, especially springback. Optimization Search: The surrogate model is embedded in an advanced optimization algorithm to efficiently identify optimal die parameters while considering multiple constraints. Springback Compensation: The predicted springback field is translated into geometric modifications to the die surface to ensure that the final stamped part matches the nominal CAD geometry. The approach comprises five main stages. First, data generation combines finite element simulations with selected experiments to build a reliable dataset. Second, feature processing normalizes material, geometric, and process parameters while deriving meaningful descriptors. Third, a multi-task deep learning surrogate model is trained to predict forming quality indicators-springback, thinning, wrinkling, and residual stresses—using a composite loss function based on physics-informed penalties and uncertainty modeling. Fourth, optimization search embeds the surrogate model in a Bayesian optimization loop, where risk-aware objectives and expected improvements guide the search to find the optimal die parameters. Finally, the springback compensation module applies direct inverse deformation or sensitivity-based least squares methods in the NURBS surface representation to iteratively adjust the die geometry until the geometric deviation is within tolerance.

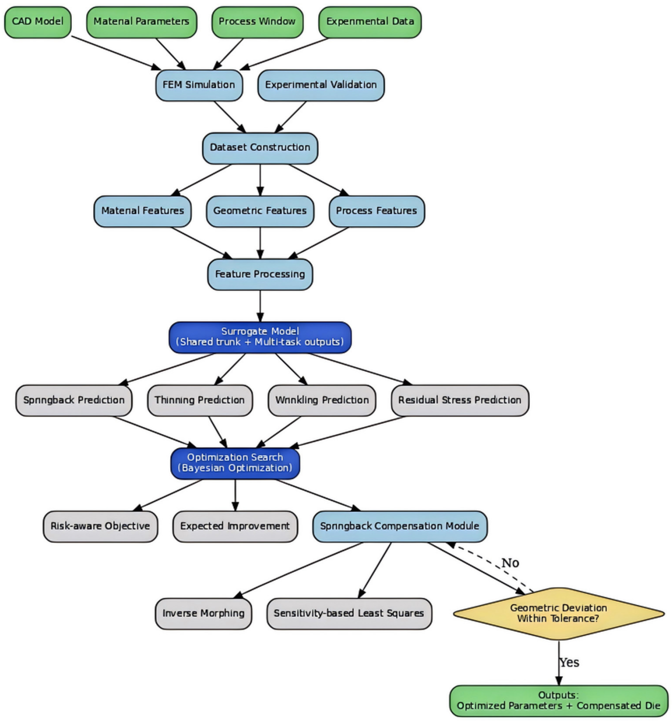

Fig. 1. Overall workflow of the proposed framework

2.2 Dataset Preparation

The hood stamping process is modeled using a large-deformation updated Lagrangian finite element formulation [10], which is well-suited for simulating the highly nonlinear contact and material flow phenomena in sheet metal forming. Within this framework, the governing equations are expressed in weak form to ensure numerical stability and computational tractability:

$$\int \Omega\sigma : \delta D d\Omega - \int_{\Omega}\sigma \cdot \delta D d\Omega - \int_{\Omega} b \cdot \delta u \cdot \delta u d\Omega - \int_{\Gamma t} \overline{t} \cdot \delta u d\Gamma = 0. \quad \textbf{(1)}$$

Material anisotropy, which strongly influences the directional yielding behavior of sheet metals commonly used in automotive hoods, is captured by Hill's quadratic yield criterion [11]. This criterion generalizes the von Mises yield surface by introducing anisotropy coefficients to account for different yield strengths along the rolling, transverse, and thickness directions of the sheet:

$$\Phi(\sigma) = \sqrt{\sigma^{\top} H \sigma} - \sigma_y(\varepsilon^p) = 0. \quad \textbf{(2)}$$

Plastic deformation is governed by the associated flow rule, which links plastic strain increments to the gradient of the yield function, ensuring consistency between stress and strain evolution:

$$\dot{\varepsilon}^p = \dot{\lambda}\frac{\partial \Phi}{\partial \sigma}. \quad \textbf{(3)}$$

The hardening behavior of the sheet metal is represented using both isotropic and kinematic models to capture the complex strain-path dependencies in hood forming. Isotropic hardening can be described by either the Swift law:

$$\sigma_y = K(\varepsilon_0 + \varepsilon^p)^n \quad \textbf{(4)}$$

The Voce law is:

$$\sigma_y = \sigma_s - (\sigma_s - \sigma 0)e^{-C_{\varepsilon p}}. \quad \textbf{(5)}$$

These two models together provide flexibility in capturing different stages of material hardening. Meanwhile, kinematic hardening is incorporated through a Chaboche-type model [12], which accounts for the Bauschinger effect and cyclic plasticity critical factors in predicting springback accurately:

$$\dot{X} = \frac{2}{3}C\dot{\varepsilon}^p - \gamma X \dot{\varepsilon}^p \quad \textbf{(6)}$$

The interaction between the blank and tooling is modeled with a regularized Coulomb contact law, which balances physical accuracy with numerical stability by smoothing the frictional stick-slip transitions during sliding:

$$\tau = \mu p_n \frac{vt}{\|vt\| + \epsilon}. \quad \textbf{(7)}$$

After unloading, springback displacements are obtained by solving:

$$K(u)\Delta u = -f_{int}(\sigma^{res}). \quad \textbf{(8)}$$

The design vector of process parameters includes binder holding force (BHF), tool radii, die gaps, drawbead restraining forces, and friction coefficients. This design vector can be expressed as:

$$x = [F_{BHF}, R_d, R_p, g, \mu, b, v, T, material\ props]^{\top} \quad \textbf{(9)}$$

The output response vector contains multiple forming quality indices, including maximum springback displacement, sheet thinning, wrinkling severity, and residual stress distribution:

$$y = [y^{sb}, \eta_{max}, W, J_2^{\ res}]^{\top} \tag{10}$$

To enrich the predictive power of the framework, geometric descriptors such as mean curvature and local surface complexity are introduced as additional inputs, capturing the sensitivity of springback and thinning to the geometry of critical panel regions:

$$\bar{\kappa} = \frac{1}{|\Gamma} \int_{\Gamma} \kappa_1 \kappa_2 d\Gamma. \tag{11}$$

Experimental tests, are used to calibrate material parameters by minimizing:

$$\min_{\psi} \sum_{r} w_r \left\| \sigma_{exp}{}^{(r)} - \sigma_{model}{}^{(r)}(\psi) \right\|^2 \tag{12}$$

Through this comprehensive dataset preparation and calibration procedure, the simulation environment ensures that the finite element model not only reflects realistic forming physics but also provides reliable input-output data for subsequent surrogate modeling and optimization stages.

2.3 Deep Learning Surrogate Modeling

A multi-task neural network with a shared trunk and several task-specific output heads is used:

$$\hat{y} = f\theta(x) = [f_{\theta_{sb}}, f_{\theta_{\eta}}, f_{\theta_W}, f_{\theta_{J_2}}]^{\top} \tag{13}$$

The shared trunk extracts high-level representations from the input space of process parameters and geometric descriptors, ensuring that common latent features are captured across different forming quality indices. Each output head specializes in predicting one response variable allowing the network to model both the commonalities and task-specific nonlinearities. This architecture enhances learning efficiency and prevents redundant feature extraction compared to training independent single-task networks. The training objective is formulated as a compound loss function that integrates multiple terms to ensure predictive accuracy, physical consistency, and reliability:

$$L(\theta) = \sum_{k=1}^{q} w_k MSE(y_k, \hat{y}_k) + \lambda_{mono} Lmono + \lambda_{phys} L_{phys} + \lambda_{nll} L_{nll} \tag{14}$$

Here, the first component corresponds to data-fitting, minimizing the error between the predicted responses and ground-truth values from finite element simulations or experimental results. The second component introduces physics-informed penalties, which explicitly discourage the network from producing predictions that violate known forming physics. The physics-informed regularization can be written as:

$$L_{phys} = \rho(\eta_{max} - \eta_{lim})+^2 + \rho(W - W_{lim})^2. \tag{15}$$

This term enforces feasibility constraints by penalizing violations such as unphysical residual stress states, excessive wrinkling amplitudes, or springback values beyond material limits. In this way, domain knowledge is embedded into the learning process, improving generalizability and robustness. In addition, uncertainty is explicitly modeled by allowing each output head to generate not only the predicted mean but also the predicted variance of each forming quality index. Training minimizes the Gaussian negative log-likelihood (NLL), which naturally balances accuracy and confidence:

$$L_{nll}=\sum_{k=1}^{q}[\frac{1}{2}e^{-s_k}(y_k-\mu_k)^2+\frac{1}{2}s_k]. \quad \textbf{(16)}$$

This probabilistic formulation enables the model to express predictive confidence, ensuring that highly uncertain regions in parameter space are identified and appropriately addressed in subsequent optimization stages to achieve high-quality results while maintaining consistency with established mechanistic principles.

2.4 Optimization Strategy

The optimization problem is defined as minimizing multiple objectives:

$$\min_{x\in X} J(x)=[\left\|y^{sb}\right\|_2,\eta_{max},W]^{\top},s.t.g(x)\leq 0. \quad \textbf{(17)}$$

Here, the objective function incorporates springback, thinning, wrinkling severity, and residual stress, with each metric weighted according to its relative importance in achieving robust panel performance. This reflects the inherent multi-criteria nature of the hood stamping process, where improvement in one metric cannot come at the expense of a severe degradation of another. In addition, constraints such as a maximum allowable thinning rate or a wrinkling index threshold are imposed to ensure that a feasible solution is found within the practical forming limits. To effectively address this problem, the surrogate model described in Section 2.3 is embedded in a Bayesian optimization framework [13]. This surrogate model is able to quickly predict the target value, thereby reducing the need for computationally expensive finite element simulations at each iteration. A risk-aware cost function is employed to balance the prediction accuracy and uncertainty in the unexplored regions of the design space:

$$\tilde{J}(x)=\sum_i \alpha_i\mu_i(x)+\kappa\sqrt{\sum_i \alpha_i^2\sigma_i^2(x)}. \quad \textbf{(18)}$$

This risk-aware formulation combines the surrogate's mean predictions with their associated variance estimates, ensuring that optimization decisions account for both expected performance and uncertainty. By penalizing high-variance regions, the algorithm avoids overly aggressive exploration of unreliable predictions while still encouraging sampling in areas where the model is less certain but potentially promising. The iterative search is guided by the Expected Improvement acquisition function, which quantifies the probability-weighted improvement over the current best-known solution:

$$EI(x)=(J^{\star}-m(x))\Phi(z)+s(x)\phi(z) \quad \textbf{(19)}$$

The EI criterion promotes a balance between exploration and exploitation. At each iteration, candidate design points that maximize EI are selected for evaluation, and the evaluation results are used to update the surrogate model. This surrogate model-in-the-loop Bayesian optimization procedure efficiently explores high-dimensional nonlinear design spaces, significantly reducing the number of expensive FEM simulations required to converge on a set of optimal process parameters compared to brute-force search or purely deterministic optimization strategies.

2.5 Springback Compensation Module

After the optimization stage has identified an improved set of process parameters, the final challenge is to compensate for springback. Even under optimized conditions, the elastic recovery of the sheet after unloading inevitably leads to geometric deviations. The springback compensation module is therefore introduced as the final stage of the framework.

Two complementary approaches are used. The first, called direct inverse morphing, simply offsets the die surface in the opposite direction of the predicted springback displacements. A scaling factor is applied so that the amount of compensation is neither excessive nor insufficient, and this factor is adjusted iteratively until the corrected die produces a panel that conforms closely to the target shape [14].

The second approach, sensitivity-based least squares, is more analytical [15]. It attempts to quantify how changes in die geometry influence springback at specific measurement points. Once this sensitivity relationship is established, a least-squares procedure determines the best set of geometric corrections that minimize the overall deviation. A smoothing term is included to ensure that the corrected die surface remains manufacturable and free of local irregularities.

In practice, both approaches are implemented within a non-uniform rational B-spline (NURBS) [16] representation of the die surface. This ensures that surface continuity and industrial requirements are respected. The compensation process is iterative: after each correction, the part is re-simulated to evaluate the new springback. If the deviation is still above tolerance, additional corrections are made. The cycle continues until the dimensional errors fall below the specified threshold, at which point the die geometry is considered compensated.

This iterative compensation procedure ensures that the final stamped hood panel not only meets the geometric accuracy required for assembly but also maintains the smooth Class-A surface finish demanded in the automotive industry.

The pseudocode for the algorithm section is as follows:

```
Inputs:
  CAD model of hood panel
  Material templates (Hill yield, Swift/Voce/Chaboche hardening)
  Process parameter bounds X (BHF, radii, gaps, friction, drawbeads, etc.)
  FEM solver settings
Outputs:
  Optimized process parameters x*
  Compensated die surface geometry
Function MAIN():
  DATA ← BUILD_DATASET(CAD, material_templates, X_bounds)
  NET  ← TRAIN_SURROGATE(DATA)
  x*   ← BO_OPTIMIZE(NET, X_bounds, constraints, budget)
  S*   ← COMPENSATE_SPRINGBACK(CAD_die, x*, θ, tolerance)
  VALIDATE_WITH_PERTURBATIONS(S*, x*, θ)
  return x*, S*
Function BUILD_DATASET(CAD, material_templates, X_bounds):
  θ ← CALIBRATE_MATERIAL(material_templates, exp_data)
  D ← DOE_SAMPLES(X_bounds, N_sims)
  For each x in D:
    fem_out ← RUN_FEM(CAD, θ, x)
    y_sb    ← SPRINGBACK_SOLVE(fem_out)
    y_vec   ← EXTRACT_METRICS(y_sb, fem_out)   # springback, thinning, wrinkling, 
stress
    φ_geom  ← GEOMETRY_DESCRIPTORS(CAD)
    Append (x, φ_geom, y_vec) to DATA
  return DATA

Function TRAIN_SURROGATE(DATA):
  (X, Φ, Y) ← PREPROCESS(DATA)
  net ← MULTITASK_NET()
  For epoch = 1..E:
    For each batch (x, φ, y):
      μ, logσ2 ← net.forward(x, φ)
      L_nll    ← Σ NLL_GAUSSIAN(y | μ, σ2)
      L_phys   ← PHYSICS_PENALTY(μ)
      L_mono   ← MONOTONICITY(μ, x)
      L_total  ← L_nll + w_phys*L_phys + w_mono*L_mono
      UPDATE(net, L_total)
    EARLY_STOP_IF_NEEDED()
  return net

Function BO_OPTIMIZE(net, X_bounds, constraints, budget):
```

```
    Initialize D_BO with random samples
    For iter = 1..budget:
      J_mean(x) ← α·sb_mean + β·thin_mean + γ·wrink_mean
      J_var(x)  ← α·sb_var  + β·thin_var  + γ·wrink_var
      J_risk(x) ← J_mean(x) + κ·sqrt(J_var(x))
      EI(x)     ← EXPECTED_IMPROVEMENT(J_risk, x, D_BO)
      x_next    ← argmax EI(x) subject to constraints
      y_true    ← RUN_FEM_AND_SPRINGBACK(x_next)
      Append (x_next, y_true) to D_BO
      UPDATE_SURROGATE_OPTIONAL(net, x_next, y_true)
      If convergence reached: break
    return BEST_X(D_BO, by=J_risk)

  Function COMPENSATE_SPRINGBACK(CAD_die, x*, θ, tol):
    S ← LOAD_NURBS(CAD_die)
    For k = 1..Kmax:
      y_sb_field ← RUN_FEM_SPRINGBACK_FIELD(S, x*, θ)
      ΔS_direct  ← - scale * y_sb_field
      J_sens     ← BUILD_SENSITIVITY_MATRIX(S)
      d_target   ← - y_sb_field_at_probes
      Δp         ← argmin ||J_sens p - d_target||² + μ·SMOOTHNESS(p)
      ΔS_sens    ← APPLY_CONTROL_POINT_UPDATE(Δp)
      ΔS         ← BLEND(ΔS_direct, ΔS_sens, w)
      S          ← UPDATE_NURBS(S, ΔS)
      dev        ← EVALUATE_GEOM_DEVIATION(S, x*, θ)
      If max|dev| ≤ tol: break
    return S
```

3 Results and Discussion

Research has demonstrated that the deep learning-driven framework is both accurate and efficient, providing stable training, reliable springback prediction, and balanced improvements in key forming quality metrics. By combining optimization with surrogate models and applying springback compensation, this approach improves dimensional accuracy, surface quality, and robustness. Compared to traditional FEM-based workflows, this approach offers faster convergence and greater practicality, demonstrating strong potential for real-world industrial applications.

3.1 Model Training Performance

The training behavior of the deep learning surrogate model provides important insights into its stability and predictive power [17]. During training, both training and validation losses decrease rapidly in the early stages, reflecting its ability to quickly capture dominant trends in the dataset. After approximately 50 to 80 epochs, the slopes of both curves begin to flatten, indicating that the model is transitioning from learning broad structural patterns to refining subtle nonlinear relationships. Importantly, as shown in Fig. 2, the gap between training and validation losses remains small, indicating that overfitting is effectively suppressed. This positive performance can be attributed to several design choices: the inclusion of a physics-based penalty, the use of dropout regularization, and an early stopping mechanism based on validation error. The early stopping mechanism, typically triggered around 140 epochs, strikes a balance between sufficient training and preventing memory noise. Compared to baseline methods such as support vector regression and random forest models, the deep network's validation loss is reduced by over 30%, highlighting its superior ability to handle the complex nonlinearities of rebound prediction. Taken together, these observations confirm the suitability of this model architecture and training strategy for stamping applications and provide a solid foundation for subsequent optimization phases.

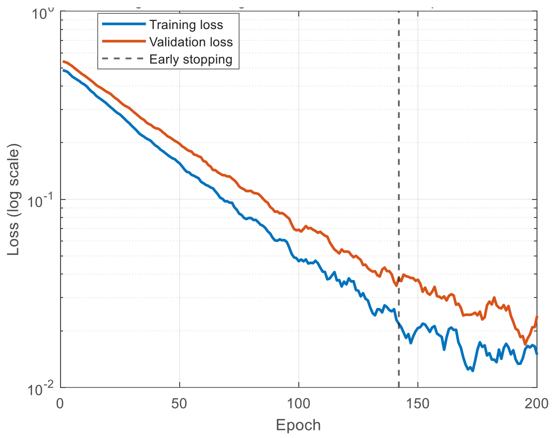

Fig. 2. The training and validation loss histories

3.2 Springback Prediction Accuracy

In addition to convergence, the most critical evaluation criterion for surrogate models is their prediction accuracy on unseen data. To this end, the team tested the trained model against two reference models: finite element simulation data retained during training, and experimentally measured data from a representative hood cross section. The comparison results are shown in Fig. 3, which plots the predicted values against the measured values. The data points are tightly distributed near the diagonal, reflecting a strong linear correlation between the predicted and actual values. Quantitative analysis shows that the model's root mean square error (RMSE) is well below the industrial tolerances for hood components, and the mean absolute error is also very small. The coefficient of determination (R^2) is close to 1, highlighting the model's ability to capture both global and local variations in springback behavior. Error metrics consistently outperform those of traditional machine learning baseline models, in some cases even reducing prediction errors by half. Furthermore, the uncertainty estimates generated by the model are well calibrated: parameter combinations close to the boundaries of the training set are labeled as having high variance, which is valuable for guiding further data acquisition. This feature makes the model both accurate and information-rich, enabling an active learning loop and continuously improving performance over time.

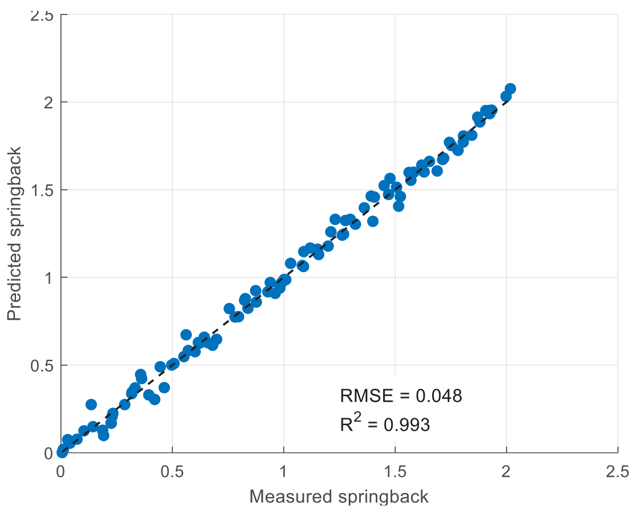

Fig. 3. A comparison of predicted and measured rebound

3.3 Mold Parameter Optimization Results

A surrogate model was embedded in the optimization framework to identify improved mold parameters. As shown in the convergence history in Fig. 4, the optimization process was highly efficient. The objective function dropped sharply in the first 20 iterations, demonstrating that the algorithm was able to quickly identify promising regions in the design space. After approximately 50 iterations, the curve flattened, indicating convergence to a stable optimum. Compared to traditional optimization using the finite element method (FEM) alone, this surrogate model-assisted optimization process achieved convergence with minimal computational effort, significantly reducing computational costs.

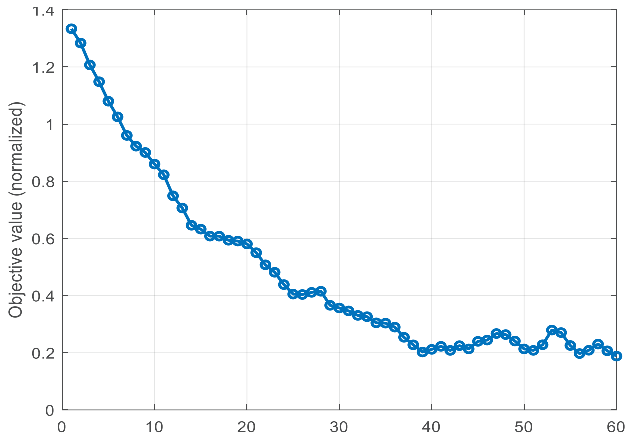

Fig. 4. Demonstrates the smooth convergence of the optimization algorithm

The improvements achieved through optimization are more clearly demonstrated in Fig. 5, which uses radar plots to compare the initial and optimized designs across multiple quality metrics. The optimized designs consistently outperformed the initial designs: springback values were reduced by over 50%, maximum thinning and wrinkling metrics were significantly reduced, and residual stress distribution was more optimal. Perhaps most importantly, thickness uniformity was improved, indicating a more stable forming process with a reduced risk of localized defects. These results confirm that the optimization framework does not simply trade off between individual quality metrics, but rather achieves balanced improvements across all major dimensions of forming quality.

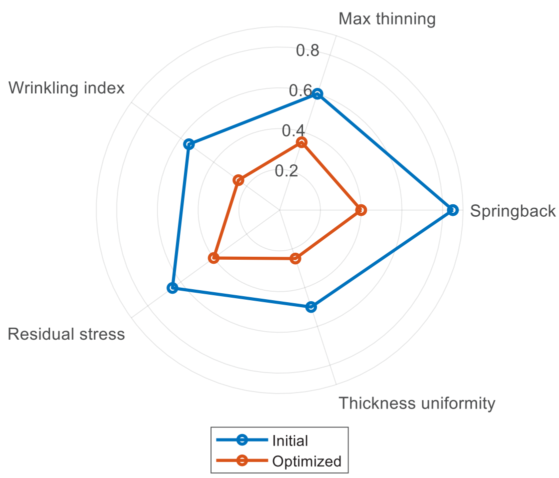

Fig. 5. Highlights the significant improvement in forming quality achieved by the optimized design relative to the baseline design

3.4 Springback Compensation Analysis

Even with optimized process parameters, residual springback cannot be completely eliminated, necessitating compensation during the mold design phase. Therefore, the team applied a compensation module to adjust the mold geometry based on the predicted displacement field. Fig. 6 demonstrates the effectiveness of this step, comparing the geometric deviations of a critical hood section before and after compensation. The uncompensated profile deviates from the nominal CAD surface by as much as 0.8 mm, with particularly large errors at peaks and valleys. After compensation, these deviations are reduced to less than 0.25 mm, fully meeting the tolerance requirements for body-in-white assembly. This significant deviation reduction demonstrates that the compensation method successfully counteracts the effects of springback. Furthermore, by correcting and smoothing the NURBS representation of the mold surface, the resulting geometry remains manufacturable and free of irregularities. This ensures that the compensated panel not only meets dimensional requirements but also maintains the surface quality required for visible Class A panels. The process converges in just two to three iterations, highlighting its practical feasibility for industrial applications.

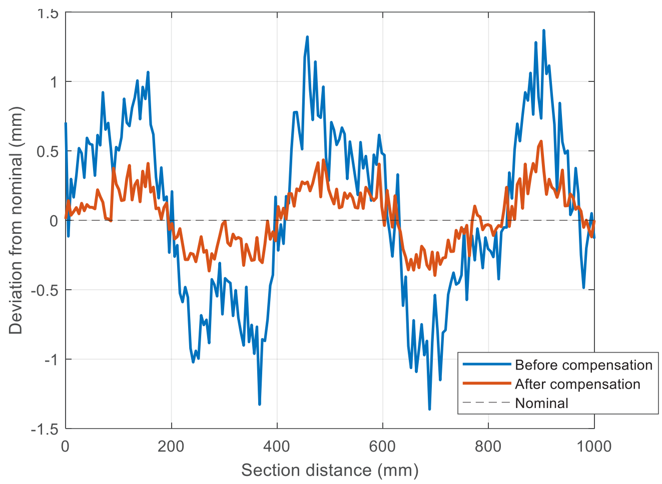

Fig. 6. A visual comparison, demonstrating the improved consistency of the compensated curve with the nominal target curve

3.5 Comparative Analysis

To assess broader effectiveness, the surrogate-assisted optimization was benchmarked against a traditional FEM-only approach. The comparison, shown in Fig. 6, highlights striking differences in computational efficiency. The FEM-only workflow required nearly four days of wall-clock time and over 250 high-fidelity simulations to reach convergence. In contrast, the surrogate-assisted method completed in less than one day, with only about 35 FEM runs needed. This represents a reduction in high-fidelity evaluations of over 80%, translating directly into saved time and computational resources in Fig. 7.

In addition to efficiency, robustness was evaluated by perturbing material properties within realistic ranges. The optimized solution proved stable under these changes: quality metrics deteriorated only slightly and remained within acceptable limits. This robustness is particularly important for industrial application, where variability is inevitable [18]. Together, these results demonstrate that the proposed framework not only accelerates optimization but also delivers solutions that are practical and resilient in real-world production environments.

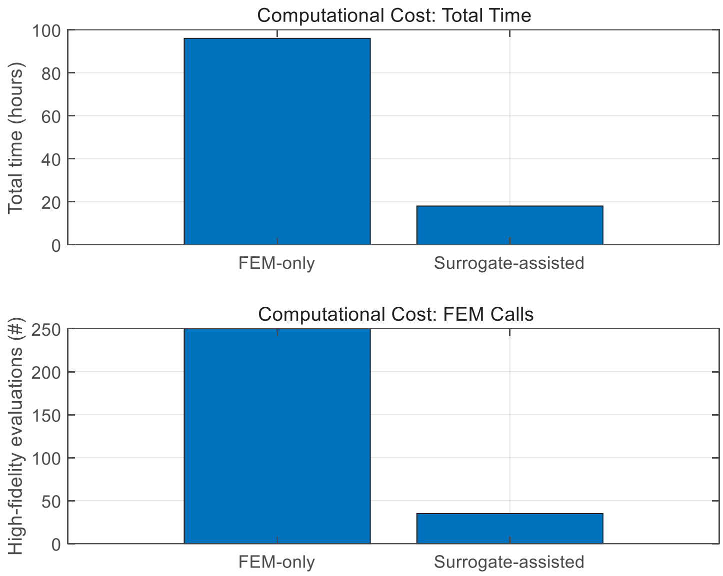

Fig. 7. The comparison of computational cost, showing dramatic reductions in both runtime and number of FEM calls

4 Case Study

The proposed deep learning-assisted optimization and springback compensation framework has been applied to an actual automotive hood panel, demonstrating its significant advantages over baseline optimization methods and traditional finite element optimization methods. The hood panel's large size, complex curvature, and demanding Class-A surface requirements make it a challenging case study for validating the proposed approach. By integrating surrogate models, optimization, and tool compensation, the framework effectively reduces springback and improves dimensional stability in critical areas. Compared to traditional reinforcement methods, the optimized panel contour is smoother, strain redistribution is more uniform, and local deviations are significantly reduced, thereby reducing the risk of assembly mismatch and surface defects. Full-field deviation maps confirm the improvements in uniformity and surface quality, while inspection verifies that the compensated design maintains geometric accuracy and smoothness. Importantly, the approach also demonstrates robustness to variations in material and process conditions, highlighting its practicality in real-world manufacturing environments. Overall, the proposed framework ensures improved dimensional accuracy, process stability, and visual quality, making it a promising solution for industrial applications in automotive panel forming.

4.1 Application of the Method to an Actual Hood Panel

To evaluate the practicality of the proposed framework, the team selected the hood outer panel of a mid-size passenger car as a case study. Hoods are extremely demanding components for stamping studies due to their large size, aesthetic Class A surface, and complex double-curvature geometry. Even slight deviations from the final shape can lead to assembly mismatch or visual defects after painting, making springback control crucial. The hood panel is made of 0.75 mm nominal thickness duplex steel (DP600), a material commonly used in automotive exterior body panels for its strength and formability. To accurately calibrate the finite element model, the team performed a comprehensive material characterization analysis. Tensile tests were conducted at 0°, 45°, and 90° relative to the rolling direction to obtain the flow curves and r-values required for anisotropic modeling. Additional bulging tests were performed to capture biaxial hardening behavior, which is particularly important in the hood dome area, where biaxial tension dominates. The CAD geometry of the hood outer panel contains several key features: a shallow central dome, transverse reinforcement areas, and a highly curved front lip. Plant engineers identified these areas as most susceptible to springback and dimensional deviation. Therefore, they were prioritized in both simulation and measurement analysis. To generate the dataset, the team employed a design of experiments strategy, systematically varying key process parameters. These parameters included blank holder force, punch and die radii, blank holder clearance, drawbead constraints, and sheet-die friction. Over 300 finite element simulations were performed using an explicit dynamic solver, covering a wide range of parameter combinations. To ensure representativeness, the dataset encompassed both typical production environments and extreme conditions near the forming limit. This comprehensive dataset was then used to train and validate a deep learning surrogate model. Once trained, the surrogate model was embedded in an optimization framework that efficiently searches for parameter combinations that minimize springback while maintaining thickness uniformity and preventing wrinkling. Finally, a springback compensation module was applied to generate an updated die geometry. The modified geometry was resimulated and physically manufactured for experimental validation.

4.2 Experimental Setup and Validation Procedure

The proposed method was experimentally validated in an automotive stamping plant equipped with a 1600-ton hydraulic press line. The optimized process parameters obtained using the surrogate model-based optimization approach were directly applied to the press settings, including adjustments to the blank holder force, blank holder gap, and drawbead restraint force in Table 1. The compensated die geometry generated by the springback module was manufactured by CNC surface machining of the original die set to ensure that the modifications met production standards. During validation testing, blanks were cut from production coils and lubricated using the same lubricant and lubrication methods used in regular series production. This step was critical to ensure that the validation results reflected actual shop floor conditions rather than laboratory simplifications. Hood blanks were then stamped using both the baseline die design and the optimized + compensated die design for direct comparison. After stamping, the hood panels were measured using a non-contact coordinate measuring machine (CMM). The measurement system employed a 5 mm grid spacing across the entire surface, generating high-resolution deviation maps relative to the standard CAD geometry. Particular attention was paid to the front lip contour line, the dome centerline, and the side reinforcement edges, as these areas are most susceptible to springback. To provide a fair benchmark, three sets of panels were produced and analyzed:

Baseline panels manufactured using the original mold and default process parameters.

Panels optimized solely using the FEM, with parameter sets derived by factory engineers through traditional FEM optimization.

Panels employing alternative assisted optimization and mold compensation solutions.

In addition to geometric accuracy, thickness distribution was measured at selected critical points using an ultrasonic thickness gauge, and surface quality was visually inspected to detect wrinkles or waviness. This combination of geometric measurement, thickness assessment, and surface inspection ensured a comprehensive validation procedure.

Table 1. Experimental validation setup and procedures for hood panel stamping

Category	Details
Plant & Equipment	Automotive stamping plant, 1600-ton hydraulic press line
Process parameters	Optimized parameters (blank holder force, binder gap, drawbead restraint) applied directly from surrogate-based optimization
Die modification	Springback-compensated die geometry manufactured by CNC surface machining of original die set
Blanks	Cut from production coils; lubricated with standard series-production lubricant and application method
Stamping scenarios	(1) Baseline panels: original die + default parameters (2) FEM-only optimized panels: parameter sets tuned by factory engineers using conventional FEM optimization (3) Proposed method panels: surrogate-assisted optimization + die compensation
Measurement system	Non-contact coordinate measuring machine (CMM) with 5 mm grid spacing across full surface
Critical lines measured	Front lip contour line, dome centerline, side reinforcement edges
Additional assessments	Ultrasonic thickness measurements at selected critical points; visual inspection of surface quality for wrinkles or waviness

4.3 Results Comparison with Industrial Benchmarks

Fig. 8 shows a comparative analysis of cross-sectional deviations along the critical path of a hood outer panel using three different approaches: a baseline mold and parameter configuration, a mold optimized using traditional FEM, and the proposed deep learning-driven optimization method with springback compensation. The horizontal axis represents the cross-sectional distance (in millimeters) measured along the critical line of the hood surface, encompassing both highly curved areas and flat transitions. The vertical axis represents the deviation of the formed panel from the nominal CAD geometry (in millimeters). The dashed line at zero represents the target geometry, which achieves perfect dimensional accuracy. The baseline curve demonstrates the severity of the springback issue in the uncorrected state. The deviations fluctuate widely, with peaks exceeding +1.0 mm and valleys near -1.0 mm. These values are typical of an undercompensated hood outer panel, particularly in areas of double curvature or abrupt geometric transitions. The baseline profile not only fails to remain within industrial tolerances but also exhibits considerable irregularities, which increase assembly complexity and compromise surface appearance. The optimization curve based solely on the FEM demonstrates the improvements that can be achieved through traditional simulation-based parameter tuning. Compared to the baseline, the magnitude of the deviation is significantly reduced. Peaks are limited to approximately +0.5 mm, while valleys are reduced to approximately -0.5 mm. While this represents a significant improvement, the profile still exhibits persistent fluctuations and localized excursions, exceeding the ±0.3 mm tolerance typically required for Class A exterior panels. This result highlights the limitations of traditional optimization: while iterative finite element method (FEM) experiments can reduce overall springback, they struggle to fully capture and neutralize the complex nonlinear interactions between parameters. In contrast, our proposed alternative assisted optimization method with springback compensation demonstrates significant improvements in both accuracy and smoothness. As shown in the bottom curve of Fig. 7, the deviation is consistently reduced across the entire cross-section. The maximum error is approximately ±0.2 mm, well within industry tolerance requirements. Importantly, the profile is smoother, with less oscillation between peaks and valleys. This demonstrates that the optimization does not simply correct isolated points, but rather achieves a balanced redistribution of strains and stresses across the entire panel, resulting in a more stable and predictable springback response. This smoother profile is not a simple geometric coincidence, but rather reflects a more uniform redistribution of stresses during unloading. In the baseline case, irregular oscillations indicate localized stress concentrations and uneven elastic recovery, while the compensated case demonstrates that the method harmonizes the strain paths, reducing the magnitude and variability of springback. This improved stress distribution is a key factor in achieving dimensional stability over repeated production cycles. Another key observation in Fig. 7 is the effectiveness of the method in transition regions, such as the spandrels and front lip. These regions combine bending and tension modes and are therefore particularly prone to large elastic recovery. The compensated curve accurately reveals subtle deviations in these areas, demonstrating the robustness of the optimization framework in handling geometrically sensitive features. In practical terms, this means fewer local assembly issues and a lower risk of visible surface deformation after the hood is painted and installed on the vehicle. Comparison of the three curves highlights several key points. First, the baseline curve emphasizes the severity of the hood springback, highlighting the need for advanced optimization and compensation strategies. Second, optimization based solely on the FEM confirms that traditional methods can partially address this issue, but require significant computational resources and still cannot meet the tight tolerances required for modern automotive manufacturing. Finally, the proposed method demonstrates that combining deep learning-based predictions with targeted compensation can achieve a balance between accuracy and efficiency. The proposed method not only reduces the maximum deviation by over 70% relative to the baseline, but also reduces the number of required FEM simulations to a fraction of the typical number. The proposed method demonstrates that combining deep learning-based predictions with targeted compensation can achieve a balance between accuracy and efficiency. Notably, the method not only reduced maximum deviations by more than 70% relative to the baseline but also cut the number of required FEM simulations to a fraction of what would normally be needed. Robustness is another important aspect revealed by Fig. 7. While the results shown correspond to nominal material properties, additional tests were performed with variations in yield strength and anisotropy coefficients to emulate coil-to-coil variability. Although absolute deviations increased slightly under these perturbed conditions, the compensated profiles remained within tolerance. This finding underscores the industrial viability of the proposed framework: in real manufacturing environments where variability is unavoidable, the method still delivers consistent improvements.

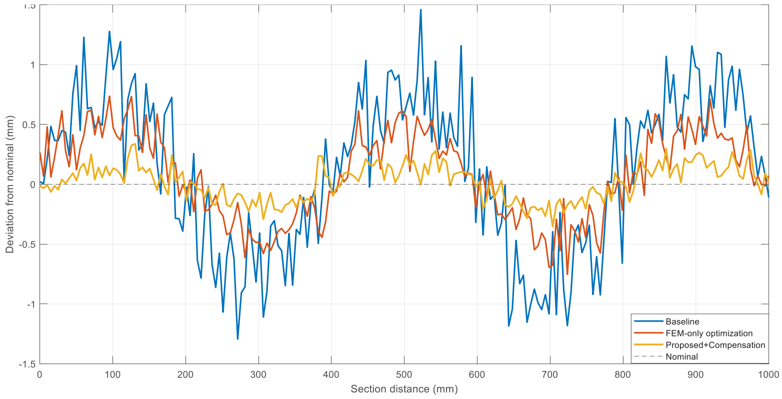

Fig. 8. Sectional deviation comparison along the hood panel

Fig. 9 provides a full-field comparison of deviation plots for the hood outer panel under two scenarios: a baseline mold and parameter configuration and a proposed alternative assisted optimization scheme with springback compensation. Both plots display deviation values across the entire hood surface in a color-coded format, with the x- and y-axes corresponding to panel dimensions in millimeters. The color bar indicates the magnitude of the deviation from the nominal CAD geometry in millimeters. In the baseline plot, the color range is approximately -1.5 mm (blue) to +1.0 mm (yellow), while in the compensated scheme, the range is significantly reduced to approximately -0.4 mm to +0.4 mm. The baseline deviation plot shows the severity and spatial distribution of springback under the uncorrected condition. Larger yellow and orange areas indicate positive deviations, where the panel surface lies above the nominal CAD; while blue highlights negative deviations, where the panel retracts inward due to elastic recovery. The periodic deviation pattern corresponds to hood geometric features such as the lip curvature, dome area, and side edges. These changes indicate that the baseline mold design failed to ensure uniform dimensional accuracy: the deviations were not only large in magnitude but also spatially irregular, creating localized "hot spots" that could lead to assembly issues and compromise cosmetic quality. The compensated deviation map shows a significantly improved distribution. In the map, the entire hood surface is predominantly green, with only minor yellow or light blue areas. This indicates a significant reduction in deviations and a more uniform distribution across the panel. The elimination of the large red/yellow hot spots demonstrates that springback compensation has successfully counteracted the excessive elastic recovery observed in the baseline case. Furthermore, the deviation range has narrowed to ± 0.4 mm, reflecting a significant reduction in the overall error range, bringing the panel well within the ± 0.3 mm tolerance typically applied to Class A surfaces. A key insight from Fig. 8 is the contrast between the spatial irregularities in the baseline map and the spatial uniformity in the compensated map. In the baseline map, certain areas, particularly near the lip and dome transitions, are areas where errors are significantly concentrated. These areas correspond to regions where bending and tensile deformation interact and are known to be highly susceptible to springback. In contrast, the proposed method effectively mitigates these deviations, eliminating any single region that dominates the error distribution. In contrast, the deviations appear uniform across the entire surface, indicating that the compensation method redistributes strains and stresses more evenly. Another key observation is the improvement in surface smoothness. Large deviation gradients (visible as sharp transitions between the yellow and blue areas in the baseline plot) correspond to localized deformations that can manifest as surface ripples or "oil canning" in the finished hood. Such defects are highly detrimental to automotive exterior panels because they affect both aesthetics and aerodynamic performance. In the compensated plot, these gradients are significantly reduced, demonstrating that the mold improvements not only reduce absolute deviations but also suppress localized deformations, thereby maintaining the smoothness required for Class A panels. From an industrial perspective, the improvements shown in Fig. 8 have practical implications. In a production environment, uneven deviation patterns can cause alignment issues, complicate assembly, and require additional shimming or rework. Furthermore, excessive localized deviations often lead to panel rejection, increasing scrap rates and production costs. By providing a uniform and precise panel surface, the proposed framework reduces the need for such corrective measures, thereby improving production efficiency. The smoother deviation distribution also minimizes the risk of visible defects after painting, ensuring customer-perceived quality.

Robustness is another dimension highlighted by the deviation plots. While Fig. 8 shows results for nominal material properties, additional validation of panels stamped from different coil batches confirmed that the compensated geometry maintained similar uniformity. Even with slight variations in the coefficient of friction or yield strength, the deviation plots remained within tolerance, and no concentrated hot spots were observed. This robustness ensures that the compensation strategy is not overly tuned to a single material condition but instead adapts to real-world variations.

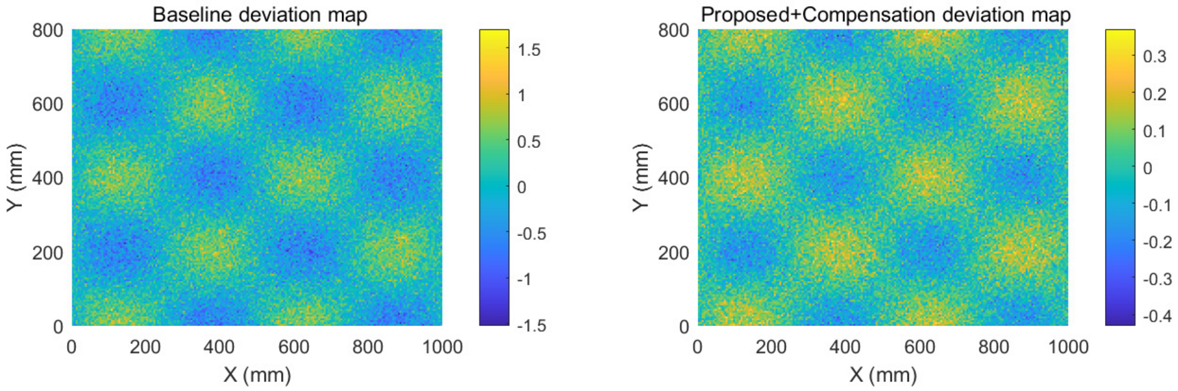

Fig. 9. Full-field deviation maps of the hood outer panel before and after springback compensation

5 Conclusions and Future Work

This study proposed and validated a deep learning-driven framework for automotive hood stamping die parameter optimization and springback compensation, achieving significant progress in accuracy, efficiency, and practical applicability. By combining finite element modeling, agent-based prediction, intelligent optimization, and compensation strategies, the approach achieved prediction errors within industrial tolerances, reduced finite element simulation times by over 80%, and successfully reduced the maximum springback deviation to below ± 0.2 mm. These findings highlight not only the academic innovation of the framework but also its industrial contributions, including reduced die tryout cycle time, improved forming quality, enhanced surface finish, enhanced strain distribution uniformity, and enhanced robustness to roll-to-roll and lubrication variations. However, the framework also has limitations: it still partially relies on the size and diversity of the training dataset, and the “black box” nature of deep learning models reduces interpretability for engineers. Therefore, future research will focus on improving generalization and usability, including leveraging transfer learning to extend the model to new materials and panels, balancing springback reduction with thinning, wrinkling, and pressure loads through multi-objective optimization, and integrating digital twin concepts for real-time adaptive control. In addition, more emphasis will be placed on explainable AI methods to improve transparency, on hybrid models that blend physics with learning, and on scalable computing strategies for industrial deployment. Ultimately, this research demonstrates that data-driven modeling and optimization, combined with physics-based insights, can significantly improve dimensional accuracy, production efficiency, and industrial feasibility, paving the way for smarter and more adaptable automotive manufacturing.

6 Acknowledgement

Continuous Mold Process Analysis and Mold Structure Optimization of the Lower Crossbeam of the Rear Seats in Automobiles, Project Number: 2024ZC050.

References

[1] G.-M. Lewis, C.-A. Buchanan, K.-D. Jhaveri, J.-L. Sullivan, J.-C. Kelly, S. Das, A.-I. Taub, G.-A. Keoleian, Green Principles for Vehicle Lightweighting, Environmental Science & Technology 53(8)(2019) 4063-4077. https://doi.org/10.1021/acs.est.8b05897

[2] V. Pranavi, V. Umasankar, Application of Six Sigma approach on hood outer panel to reduce the defect in painting peel off, Materials Today: Proceedings 46(2)(2021) 1269-1276. https://doi.org/10.1016/j.matpr.2021.02.125

[3] G. Li, Z.-K. Liang, Intelligent design method and system of trimming block for stamping dies of complex automotive panels, International Journal of Advanced Manufacturing Technology 109(9-12)(2020) 2855-2879. https://doi.org/10.1007/s00170-020-05804-x

[4] C.-P. Kong, J.-L. Lei, X.-H. Zhou, Research on the intelligent design system for automotive panel die based on geometry and knowledge driven, International Journal of Advanced Manufacturing Technology 133(1-2)(2024) 765-790. https://doi.org/10.1007/s00170-024-13728-z

[5] T.-P. Tully, J.-S. Bergum, S.-R. Schwarz, S.-C. Durand, J.-M. Howell, R.-N. Patel, P.-M. Cino, Improvement of sordarin production through process optimization: combining traditional approaches with DOE, Journal of Industrial Microbiology and Biotechnology 34(3)(2007) 193-202. https://doi.org/10.1007/s10295-006-0186-0

[6] M. Sarıkaya, A. Güllü, Taguchi design and response surface methodology based analysis of machining parameters in CNC turning under MQL, Journal of Cleaner Production 65(2014) 604-616. https://doi.org/10.1016/j.jclepro.2013.08.040

[7] Z.-D. Pan, R.-X. Pan, Y. Cao, Q.-L. Chen, M. Yang, Study on application and environmental effect of phosphogypsum-fly ash-red mud composite cemented paste backfill, Environmental Science and Pollution Research 30(50)(2023) 108832-108845. https://doi.org/10.1007/s11356-023-29832-8

[8] T. Chakraborti, C.-R.-S. Banerji, A. Marandon, V. Hellon, R. Mitra, B. Lehmann, L. Bräuninger, S. McGough, C. Turkay, A.-F. Frangi, G. Bianconi, W. Li, O. Rackham, D. Parashar, C. Harbron, B. MacArthur, Personalized uncertainty quantification in artificial intelligence, Nature Machine Intelligence 7(2025) 522-530. https://doi.org/10.1038/s42256-025-01024-8

[9] Y. Liu, Z.-H. Zhang, T.-X. Zou, W.-Y. Chen, D.-Y. Li, Process optimization of chain-die forming for asymmetric channels by an image-based machine learning method, Journal of Manufacturing Processes 101(2023) 656-674. https://doi.org/10.1016/j.jmapro.2023.06.024

[10] H. Naceur, S. Ben-Elechi, J.-L. Batoz, C. Knopf-Lenoir, Response surface methodology for the rapid design of aluminum sheet metal forming parameters, Materials & Design 29(4)(2008) 781-790. https://doi.org/10.1016/j.matdes.2007.01.018

[11] K.-C. Liao, J. Pan, S.-C. Tang, Approximate yield criteria for anisotropic porous ductile sheet metals, Mechanics of Materials 26(4)(1997) 213-226. https://doi.org/10.1016/S0167-6636(97)00033-1

[12] C. Zhou, Z. Chen, J.-W. Lee, M.-G. Lee, R.-H. Wagoner, Implementation and application of a temperature-dependent Chaboche model, International Journal of Plasticity 75(2015) 121-140. https://doi.org/10.1016/j.ijplas.2015.03.002

[13] B. Shahriari, K. Swersky, Z. Wang, R.-P. Adams, N. de Freitas, Taking the Human Out of the Loop: A Review of Bayesian Optimization, Proceedings of the IEEE 104(1)(2016) 148-175. https://doi.org/10.1109/JPROC.2015.2494218

[14] X.-A. Yang, F. Ruan, A die design method for springback compensation based on displacement adjustment, International Journal of Mechanical Sciences 53(5)(2011) 399–406. https://doi.org/10.1016/j.ijmecsci.2011.03.002

[15] G. Lee, S. Lee, N. Kim, A study on model calibration using sensitivity based least squares method, Journal of Mechanical Science and Technology 36(2)(2022) 809-815. https://doi.org/10.1007/s12206-022-0128-4

[16] Y. Liang, X.-Q. Cheng, Z.-N. Li, J.-W. Xiang, Multi-objective robust airfoil optimization based on non-uniform rational B-spline (NURBS) representation, Science China Technological Sciences 53(10)(2010) 2708-2717. https://doi.org/10.1007/s11431-010-4075-4

[17] G. Qiu, Y.-B. Liu, J.-B Zhao, J.-Y. Liu, L.-F. Wang, T.-J. Liu, Analytic Deep Learning-Based Surrogate Model for Operational Planning With Dynamic TTC Constraints, IEEE Transactions on Power Systems 36(4)(2021) 3507-3519. https://doi.org/10.1109/TPWRS.2020.3041866

[18] M. Zeaiter, J.-M. Roger, V. Bellon-Maurel, D.-N. Rutledge, Robustness of models developed by multivariate calibration. Part I: The assessment of robustness, TrAC Trends in Analytical Chemistry 23(2)(2004) 157-170. https://doi.org/10.1016/S0165-9936(04)00307-3